18TH WORLD CONFERENCE ON EARTHQUAKE ENGINEERING
WCEE2024
MILAN

MILAN, ITALY
30TH JUNE - 5TH JULY 2024

www.wcee2024.it

# EFFECT OF DAMPING IN NONLINEAR DYNAMIC ANALYSIS OF EXISTING REINFORCED CONCRETE BUILDINGS

M. Terrenzi[1], C. Cantagallo[1], G. Camata[1] & E. Spacone[1]

[1] University "G. d'Annunzio" of Chieti-Pescara - Department of Engineering and Geology

Viale Pindaro 42, 65127 Pescara, Italy

marco.terrenzi@unich.it, cristina.cantagallo@unich.it , guido.camata@unich.it, enrico.spacone@unich.it

**Abstract**: *Nonlinear Response History Analysis (NRHA) is the most accurate method for predicting the building response under strong ground motions. The results of these analyses depend on many factors such as the ground motion selection, the structural modelling strategies (frame vs solid models, lumped or distributed plasticity models) and the damping models used. The definition of the damping models and their influence on the structural response to date is one of the most complex, uncertain and least studied elements. This is partly due to the difficulties in understanding the mechanical meaning of the damping models. This paper focuses on the comparison between two of the most widely used damping models: the Modal and the Rayleigh damping. A representative Italian 6-storey existing reinforced concrete building designed for gravitational loads only is studied, with and without infills. In both cases, NRHAs are carried out using 20 pairs of ground motion records selected for a return period of 475 years. The results of the two damping approaches are compared to evaluate their impact on the overall response of the case-study building.*

## 1. Introduction

Damping in structures refers to the ability of a system or structure to dissipate or absorb energy when subjected to dynamic loads, such as vibration or oscillation. The damping capacity of the structural model can be defined as the percentage of the total vibration energy lost in one cycle. It can be of two types: hysteretic (cyclic damping or cyclic energy dissipation related to the material response) and additional damping (introduced to account for all those dissipating mechanisms that are not or cannot be accounted for by the model). In a "perfect" model where all dissipating phenomena are explicitly models, there is no need for additional damping. This paper deals with the additional structural damping, which depends on material properties and structural configuration. The overall damping is generally represented by a damping ratio, which is a measure of the relative amount of energy dissipated per vibration cycle. The damping mechanisms are usually related to friction, energy dissipated in the closing and opening cycles of concrete cracks, plastic energy dissipation in hysteretic cycles of materials, thermal energy dissipation due to heating of materials in loading and unloading cycles, etc. Currently, it is difficult, if not impossible, to explicitly model all the different sources of damping. The purpose of this paper is to analyze possible approaches to modeling additional damping in structures, quantify their effect, and provide recommendations for avoiding possible unanticipated effects. The discussion is limited to the two most popular approaches implemented in OpenSees (Mazzoni et al. 2006) software, Rayleigh damping (Rayleigh 1971, Chopra 2012) and modal damping (Wilson and Penzien 1972, Carr and Ruaumoko 2007, Chopra and McKenna 2016). The simplest and most widely used model is Rayleigh damping, where the damping matrix is proportional to a linear combination of the mass and stiffness matrices (Figure 1a). The damping matrix c is expressed as:

$$c = \alpha\, m + \beta\, k \tag{1}$$

where $m$ is the mass matrix, $k$ is the stiffness matrix, and $\alpha$ and $\beta$ are the Rayleigh damping coefficients determined from the damping ratios specified for two selected modes or two frequencies, *i* and *j*. The definition of the two modes/frequencies is done in such a way as to ensure that the damping in all modes that contribute significantly to the response are close to the target value, since values outside the range lead to higher damping ratios and thus would be overdamped.

In NRHAs, the original definition of Rayleigh damping considers $k = k_{initial}$. More recently, that have been proposals to update $k$ as the structure damages (using for example the tangent stiffness or the committed stiffness – see discussion in §4). Charney (2008) pointed out that the initial stiffness may generate an excessive damping force and recommended the utilization of tangent stiffness as an alternative. However, Chopra and McKenna (2016) warn about the use of the tangent stiffness as the physical meaning of $c$ may be lost if the tangent stiffness becomes negative definite due to softening.Another damping modeling approach is Modal damping, that uses a linear combination of mass damping and stiffness. Modal damping allows to prescribe a given damping ratio for any vibration mode (Figure 1b). Modal damping can be expressed as:

$$c = m\left(\sum_{n=1}^{N}\frac{2\zeta_n\omega_n}{M_n}\phi_n\phi_n^T\right)m \qquad (2)$$

where, $\zeta_n$ is the damping ratio at the n-th mode, $\phi_n$ is the n-th mode eigenvector and $M_n$ is the n-th mode generalized mass. All the above modal properties typically refer to the initial, linear system.

The modal damping model has the advantage of eliminating spurious damping forces.

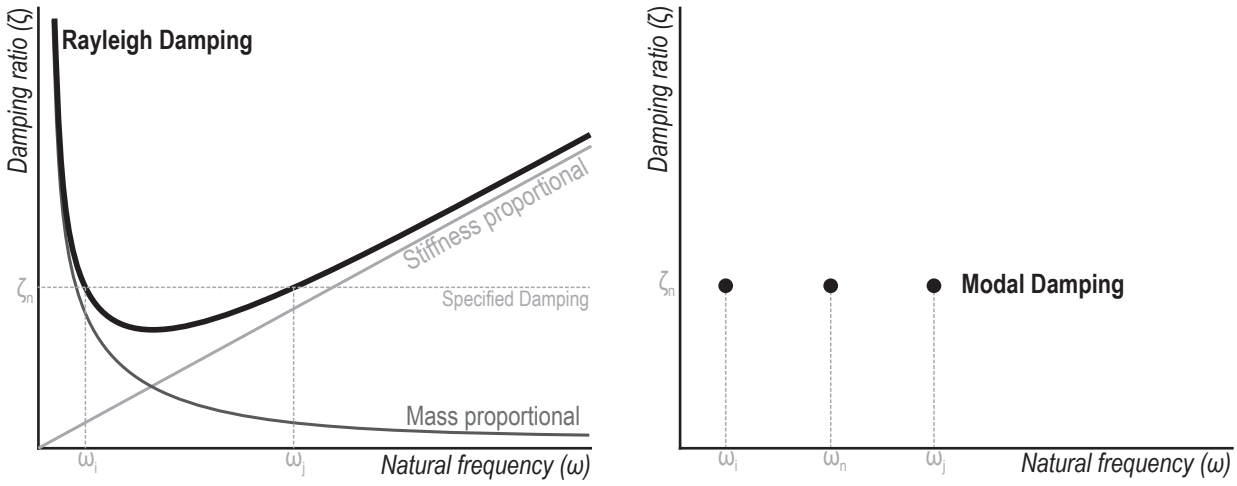


*Figure 1. Graphic representation of (a) Rayleigh Damping e (b) Modal Damping for same damping ratio at all prescribed frequencies*

The definition of damping models and its influence on the structural response needs further investigation because of its clear lack of mechanical meaning and significant impact on the structural response. This paper focuses on comparing the two most widely used damping models previously described, using 6-story Italian reinforced concrete building designed for gravity loads only, with and without infills.

## 2. Case study description

The vast majority of the Italian reinforced concrete building stock dates back to the 60s and 70s (source: Census data ISTAT (2011) and was designed without seismic prescription and/or according to outdated seismic codes. The case study building analyzed in this paper was designed for gravity loads only. It has 6 floors since a significant percentage of existing non-conforming buildings have 4 to 6 floors (Basaglia et al. 2021). The spatial configuration of the structures (Fig. 1) consists of four frames with seven bays in the X-direction and only the two external frames in the Y-direction. The inter-story height is 3.2 m. Since most beams

are aligned in the X direction, all columns also have their strong axis along this direction, leading to significantly greater total lateral stiffness and strength in the X direction with respect to the Y direction.

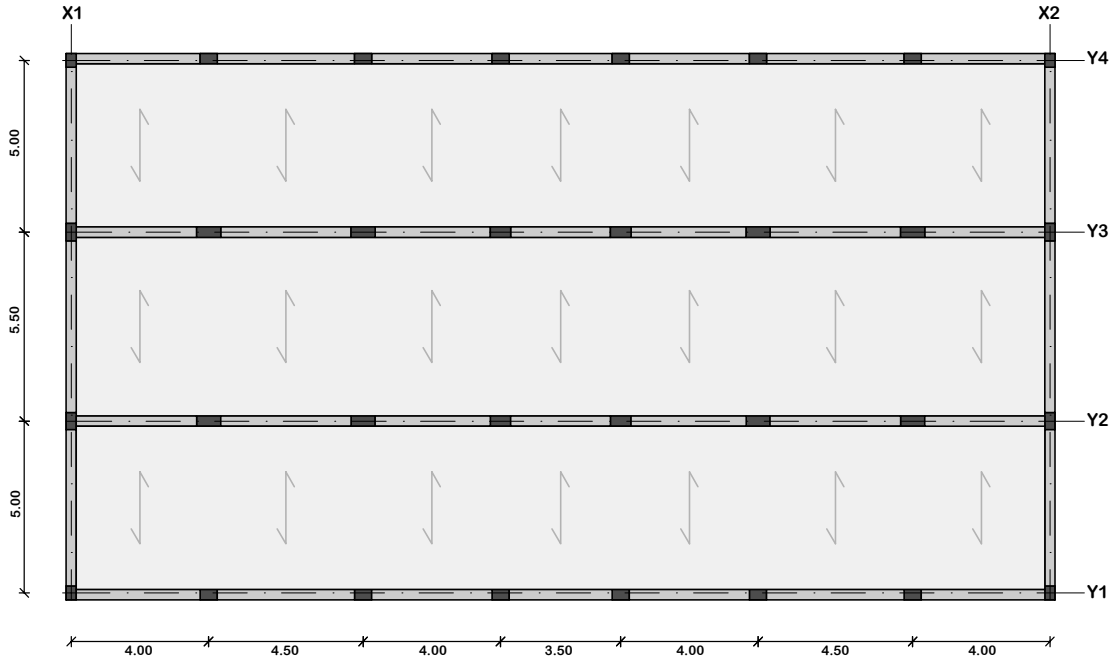


*Figure 2. Plan layout of case study building*

The cross sections and rebar layouts of columns and beams were sized according to the allowable stress design method prescribed by the Italian building standard in use in the 1970s (DM. 1974) [8]. The characteristic cubic compressive strength of concrete is $R_{ck}$ = 25 MPa, while steel grade Feb38K with a yield stress $f_{yk}$ = 375 MPa is used for all reinforcement.

### 2.1. Numerical models and modal results

The building models were created in OpenSees using the pre/post processor STKO (Petracca et al 2017). As regards the modeling of beams and columns (Terrenzi et al. 2020) a Beam-with-Hinges element modeling strategy (Scott et al. 2006) was used. This element utilizes a force-based formulation with the modified Gauss Radau integration, which restricts nonlinear constitutive behavior to specific plastic hinge regions with a defined length $L_{pl}$, modeled as fiber sections (Spacone et al. 1997), while the central part of the element has elastic sections properly calibrated to take into account cracking. Potential brittle failure in beam/column elements and/or beam-column joints are not model as this paper study focuses on damping rather than building failure. The models include P-Delta effects. The fiber sections uses Concrete01 (Kent and Park 1971) for concrete, with the same properties for confined and non-confined concrete because the stirrup spacing is too large for an effective confinement, and Steel01 (Menegotto and Pinto 1973) for steel. The plastic hinge length is calculated in a assumed equal to the section depth. In columns with rectangular sections, the average value between the two depths was used. The floor diaphragms are modeled using the MPconstraints “rigidDiaphragm”. The rigid diaphragm constraint restrains any axial deformation in the beams thus introducing spurious axial forces, typically in compression. To oercome this problem a ZeroLength element (or axial buffer element, Barbagallo et al 2020) was added one of each beam’s ends, with a low stiffness in the axial dof, in order to allow the beam to axially deform without developing spurious axial forces, and rigid links in the other degrees of freedom.

The infills were modeled with diagonal strut elements (compression only) based on the phenomenological model proposed by Decanini et al. (1987) appropriately updated according to recent enhancements by Cardone and Perrone (2015) and Sassun et al. (2016). This model describes the monotonic and cyclic behavior as a function of the mechanical and geometric characteristics of the infills thus considering the presence of the openings. The behavior model was modeled by Concrete01 (Noh et al. 2017). At ground level,

the rear frame (Y4 in Figure 2) is infilled without openings, and there are no infills on the other sides. On the other story all external frames are infilled, with percentages of openings from approximately 80% up to 0% (i.e. without openings). The structure is considered fixed at the base. Table 1 reports the results of the modal analysis of the two models, Bare Frame (BF) e Infill Frame (IF), carried out after the application of the gravity loads corresponding to 100% dead load plus 30% live load.

*Table 1. Modal parameters*

| | | Mode 1 | Mode 2 | Mode 3 | Mode 4 | Mode 5 | Mode 6 |
|---|---|---|---|---|---|---|---|
| **Bare Frame (BF)** | **T** | 2.59 [s] | 1.48 [s] | 1.20 [s] | 0.78 [s] | 0.47 [s] | 0.41 [s] |
| | **Mass** | 78.65% | 80.45% | 79.34% | 10.97% | 10.49% | 5.00% |
| | **Dir.** | Y | Rot. | X | Y | Rot. | X |
| **Infill Frame (IF)** | **T** | 0.97 [s] | 0.64 [s] | 0.53 [s] | 0.30 [s] | 0.21 [s] | 0.17 [s] |
| | **Mass** | 93.56% | 70.21% | 74.51% | 5.41% | 8.90% | 4.82% |
| | **Dir.** | Y | X | Rot. | Y | X | Rot. |

### 2.2. Ground motion record selection

The selection of ground motion records for the NRHAs was carried out considering L'Aquila (Italy) as the reference site and a seismic eventwith a return period of 475 years. The ground motion records were selected from two databases: the European Strong-motion Database ESD and the Engineering Strong-Motion database ESM. For both buildings, 20 pairs of unscaled ground motion records were selected. Further details can be found in in Cantagallo et al. (2023).

## 3. Nonlinear time history analyses w/o Damping

Based on the 20 pairs of ground motion records, NRHAs were carried out with different damping approaches, including various damping values. First, the analyses were carried out considering only the hysteretic damping of the materials, without adding any additional damping. The results of these analyses are reported in Figure 3 for both models. One Engineering Demand Parameter (EDP) was considered, i.e. the maximum displacement of the center of mass (RD) of the top floor (Terrenzi et al. 2022). It can be observed that for some analyses, the displacements are very high, especially in the weaker Y direction. These cases refer to analyses that did not converge, as indicated in Figure 3 with an unfilled marker. The pairs of ground motion records that converged totaled 14 for both the BF and IF models. It is worth noting that the selection of ground motion records was different for the two models, so the equal number of convergent ground motion pairs records was coincidental. Since the objective is not to perform an assessment but to compare different damping approaches, it was decided to continue the study using the 14 convergent pairs of ground motion records, excluding the 6 non-convergent ones.

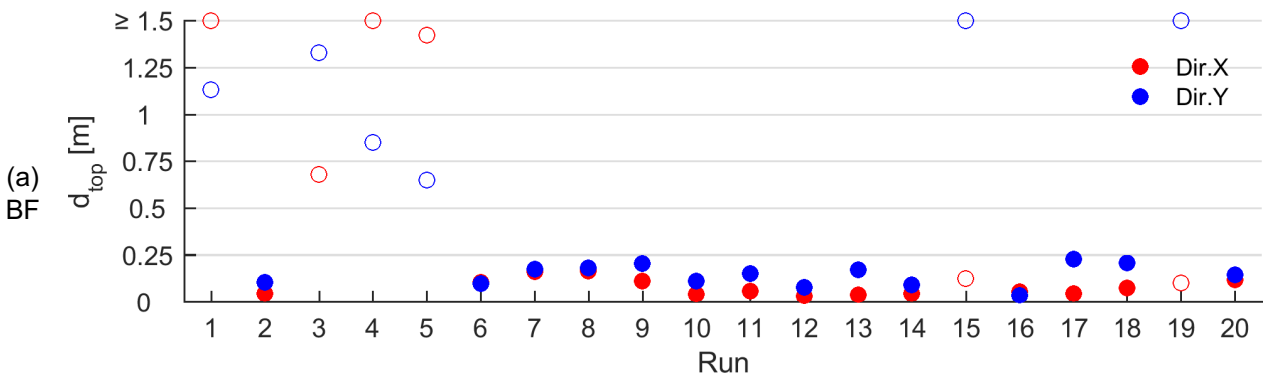

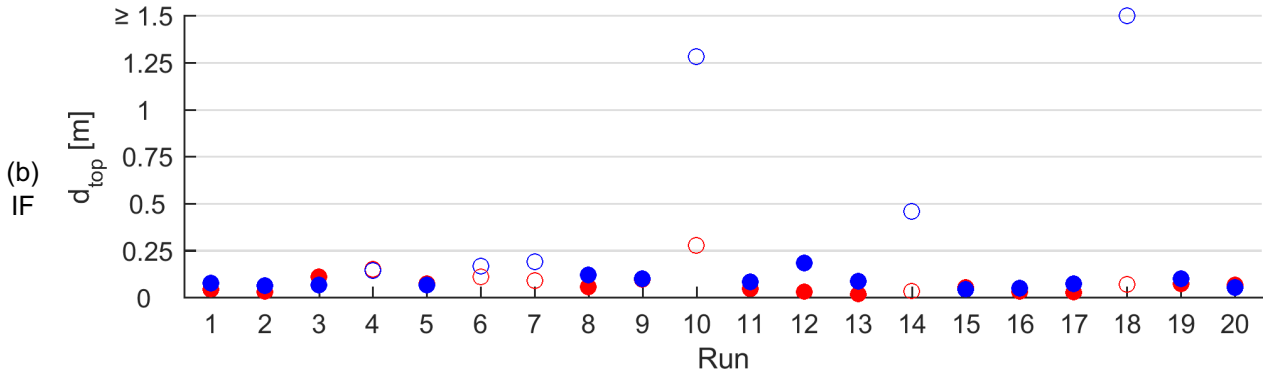


*Figure 3. – Bare Frame (a) and Infill Frame (b): Results of NRHAs in terms of maximum Roof Displacement in the X and Y directions (Red marker for X direction, Blue marker for Y direction, with filled markers indicating converged analyses and empty markers indicating non-converged analyses)*

## 4. Nonlinear time history analyses with Rayleigh damping

The first damping model used is the commonly used Rayleigh damping model. Three different approaches are available in OpenSees, which differ for the stiffness matrix used, which can be the initial stiffness, the current or tangent stiffness, or the committed stiffness. In this work the initial $K_{init}$ and the committed stiffness $K_{comm}$ were used, the latter defined as follows. During the iterations at the structural (global) level, the stiffness matrix may change at each iteration (current or tangent). When global convergence is reached, the last computed stiffness matrix is saved and labeled committed $K_{comm}$. When Rayleigh damping with $K_{comm}$ is used, the damping matrix does not change during the iterations of a load step and is updated when convergence is reached. This approach allows for a lower computational effort than using the current stiffness where the stiffness matrix is updated at each iteration. Furthermore, given that the current stiffness may be unstable and refers to a non-converged point, its physical meaning may be lost. It is worth pointing out that even though K is updated, $\alpha$ and $\beta$ are not updated to provide $\zeta_n$ in the new frequencies. Two approaches for specifying the Rayleigh damping ($\zeta_n$) were used: the first mode is the fundamental mode of the structure, and the second mode is the last mode with significant participating mass ($M_n \geq 5\%$), which, for both models (BF and IF), coincides with the 6$^{th}$ mode. The analyses were carried out for $\zeta_n$ ranging from 1% to 5% (with 1% increments). The results for the BF model reported in Figure 4 show that the contribution of Rayleigh damping at the same $\zeta_n$ is more significant in dir. X than in dir.Y. Using $K_{init}$ shows lower RDs in dir.X than the same analyses with $K_{comm}$. The trend lines show how the differences between $K_{init}$ and $K_{comm}$ become more significant as $\zeta_n$ increases.

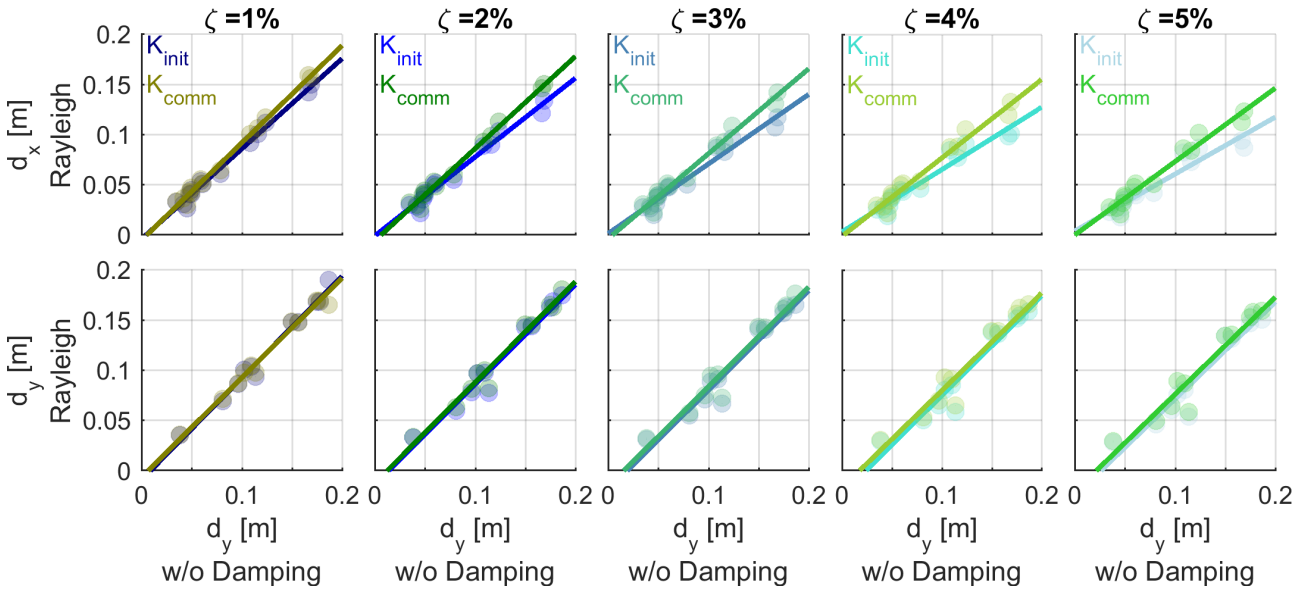


*Figure 4. NRHAs of the BF model with Rayleigh damping: maximum RD in the X and Y directions with trend lines (only 14 convergent ground motion records are included)*

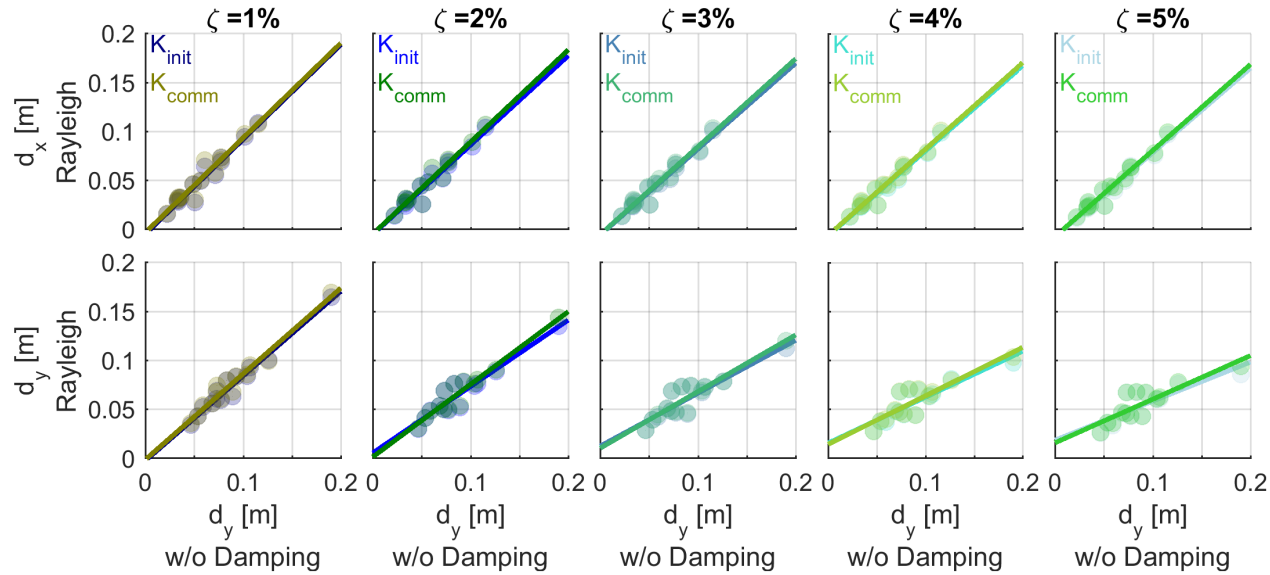


*Figure 5. NRHAs of the IF model with Rayleigh damping: maximum RD in the X and Y directions with trend lines (only 14 convergent ground motion records are included)*

In the Y-, weaker direction these differences in terms of trend lines are less pronounced and nearly negligible. For the IF model (Figure 5), the differences between Rayleigh damping with $K_{init}$ and $K_{comm}$ as shown by the trend lines are negligible on average and remain unchanged as $\zeta_n$ increases. This is probably due to the fact that the inelastic demand is much smaller in the IF model, thus the difference between $K_{init}$ and $K_{comm}$ is less significant that in the BF case. Unlike the BF building, the contribution of Rayleigh damping is more significant in dir.Y than in dir.X.

## 5. Nonlinear time history analyses with Modal Damping

The other approach used is Modal Damping. Similarly to Rayleigh damping, the analyses were carried out for $\zeta_n$ ranging from 1% to 5%, with the same damping ratio imposed on the first 6 modes.

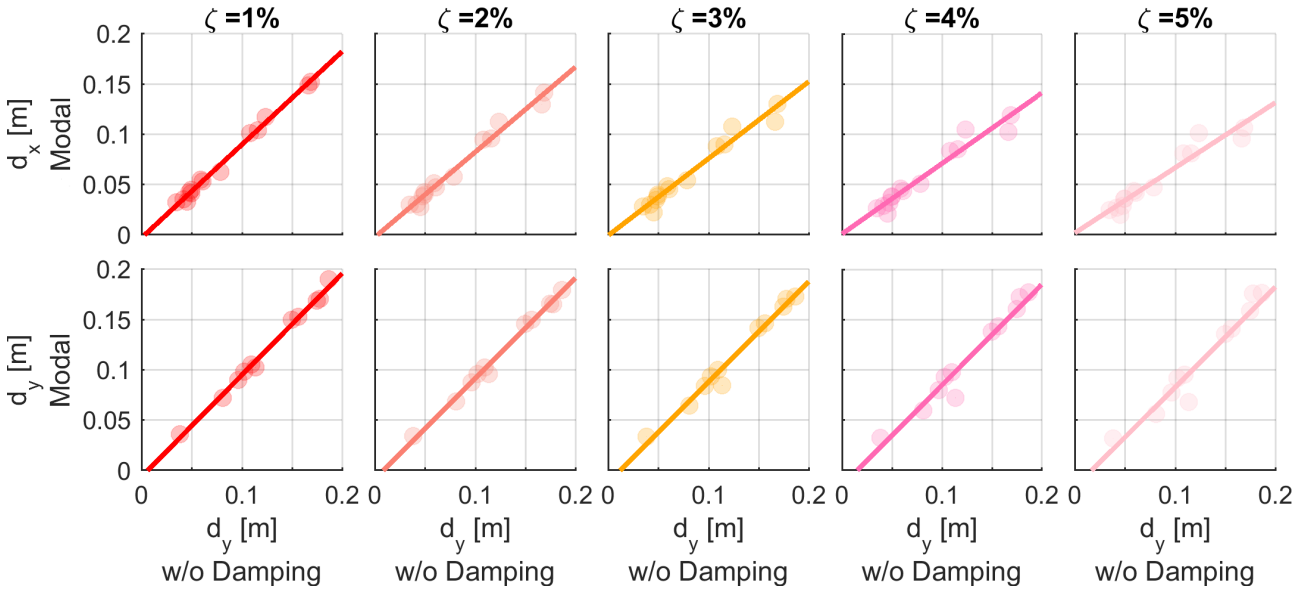


*Figure 6. NRHAs of the BF model with Modal damping: maximum RD in the X and Y directions with trend lines (only 14 convergent ground motion records are included)*

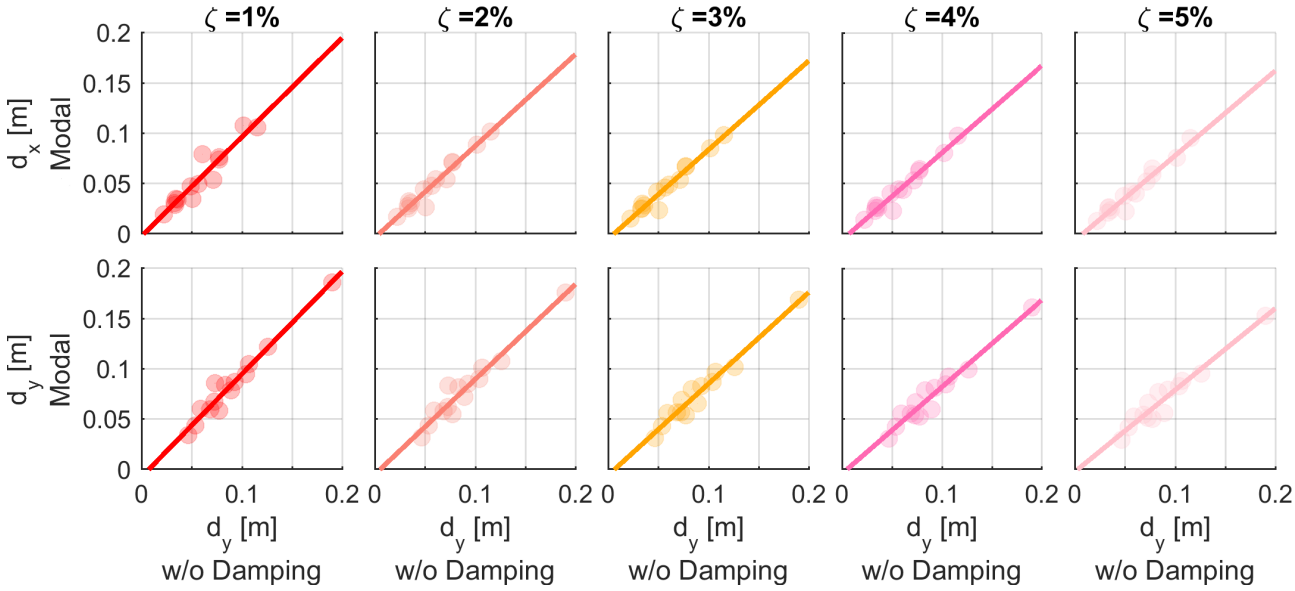


*Figure 7. NRHAs of the IF model with Modal damping: maximum RD in the X and Y directions with trend lines (only 14 convergent ground motion records are included)*

The results on the BF building in Figure 6 show that the contribution of Modal Damping at the same $\zeta_n$ is more significant in dir. X, than in the weaker dir. Y. On the IF building in Figure 7, on the other hand, the contribution of damping seems to be similar in the two directions.

## 6. Rayleigh damping Vs. Modal Damping

The analyses with the two damping approaches were compared in terms of max RD in the two directions for both models of the 6-story building. In the BF model, as shown in Figure 8, it can be observed from the trend lines that fit the results that the differences between Modal Damping and Rayleigh Damping with $K_{init}$ and $K_{comm}$ are minimal and tend to increase with $\zeta_n$.

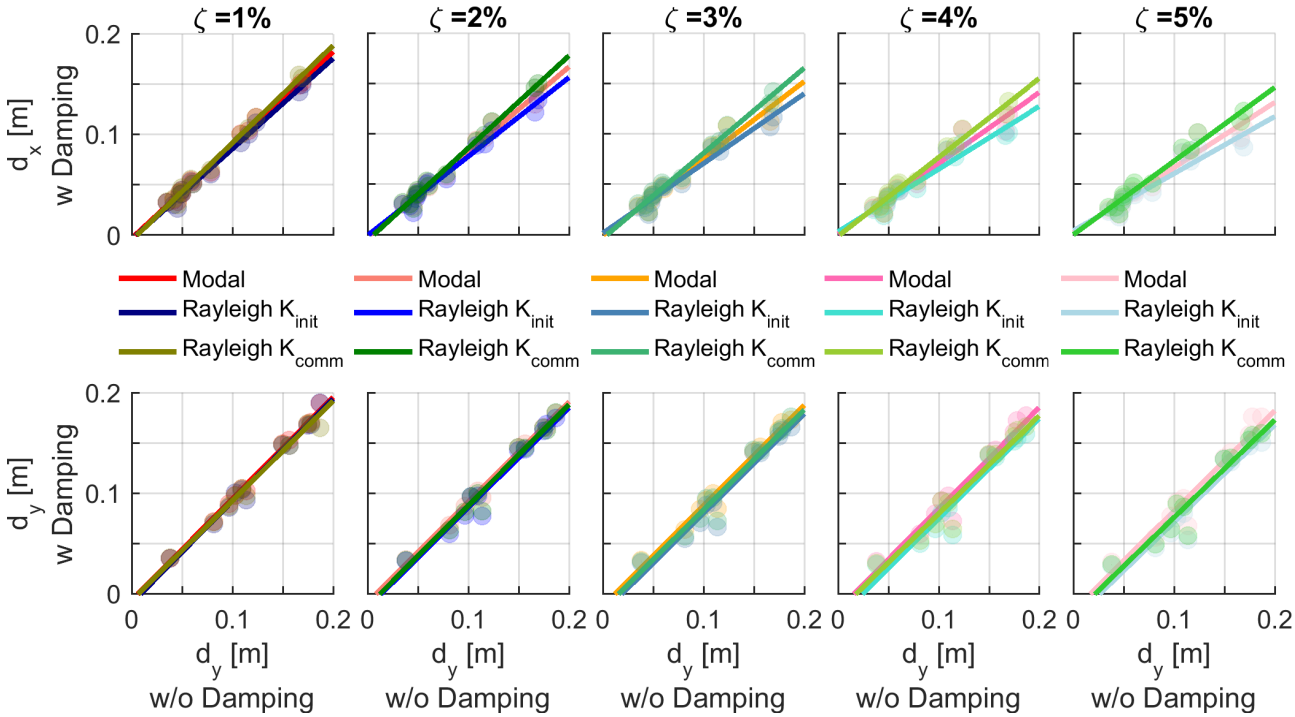


*Figure 8. Comparison of NRHAs for the BF model between Rayleigh and Modal Damping in terms of maximum RD in the X and Y directions (with trend lines)*

In the X-direction, the strong direction, there is a greater difference between the damping approaches, with Modal Damping positioned in an intermediate condition between Rayleigh Damping with $K_{comm}$ and Rayleigh Damping with $K_{init}$. In the Y-direction, the weak direction, the trend lines overlap, indicating that the results are generally similar. In the IF model, as seen in Figure 9, in the X-direction, the trend lines overlap, indicating that the results are generally similar between Modal and Rayleigh Damping with $K_{init}$ and $K_{comm}$. However, in the Y-direction, differences are observed between Modal and Rayleigh Damping, which tend to increase with $\zeta_n$. More specifically, it can be noted that Modal Damping exhibits lower damping compared to Rayleigh Damping

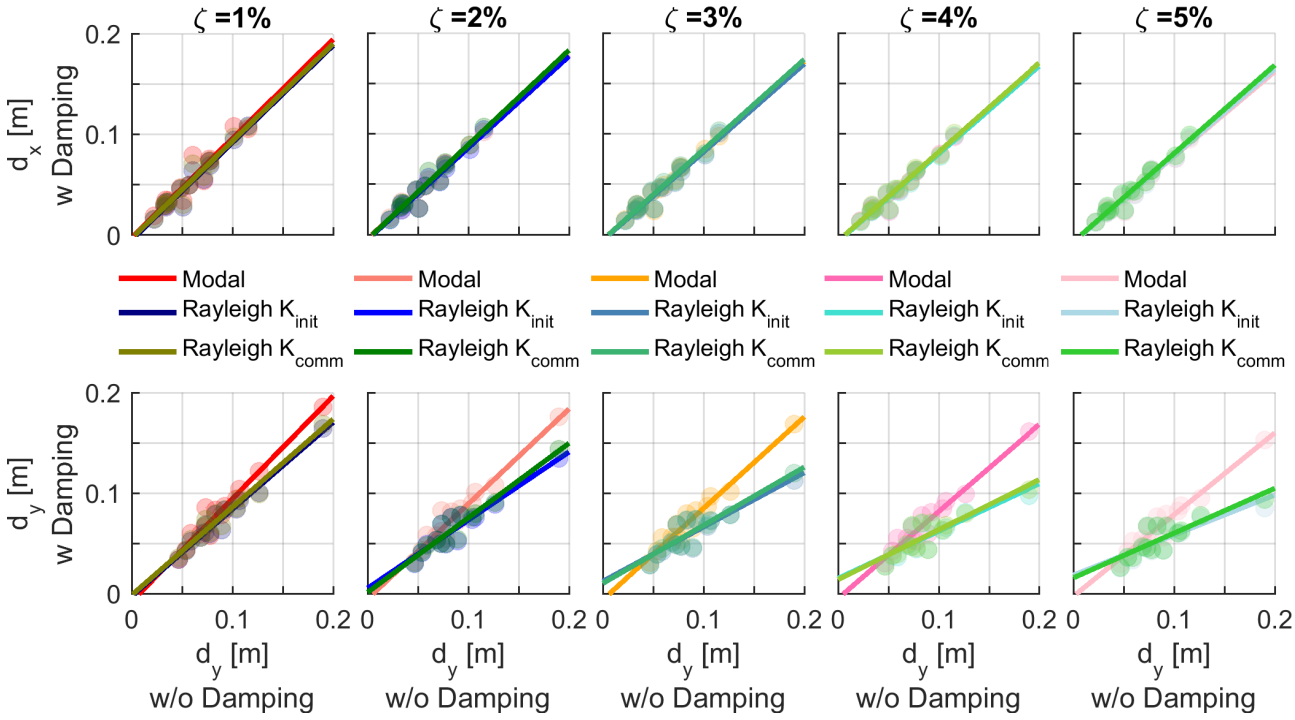


Figure 9. Comparison of NRHAs for the IF model between Rayleigh and Modal Damping in terms of the maximum RD in the X and Y directions (with trend lines)

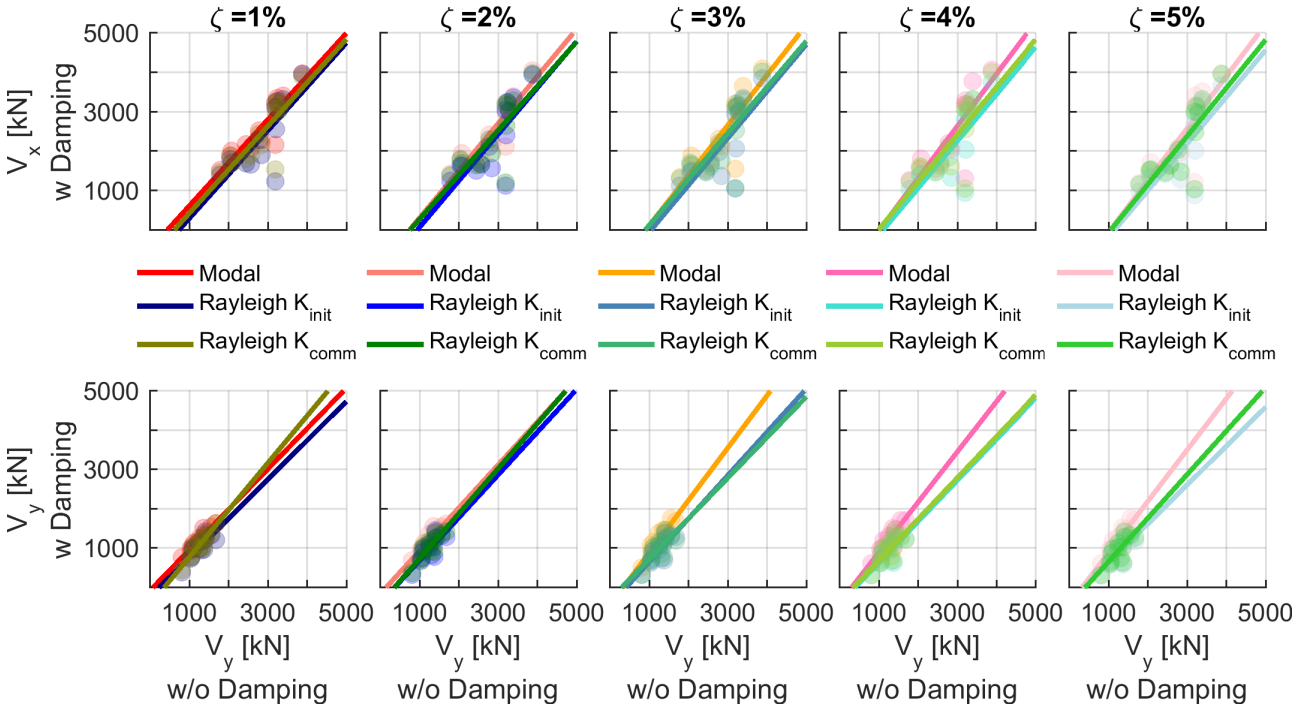


*Figure 10. Comparison of NRHAs for the BF model between Rayleigh and Modal Damping in terms of the maximum base shear in the X and Y directions (with trend lines)*

Additional comparisons were carried out using the maximum base shear $V_y$ as the EDP. In Figure 10, for the BF building, the trend lines that fit the results are close to each other. As $\zeta_n$ increases, the differences between Modal Damping and Rayleigh Damping with $K_{init}$ and $K_{comm}$ tend to increase. In the strong direction (X), Modal Damping provides lower damping than Rayleigh Damping with $K_{init}$ and $K_{comm}$. On average, it exhibits base shear values that are comparable to the approach using only hysteretic material damping. In the Y-direction, the approach with Modal Damping shows higher averagely base shear values compared to the analyses w/o damping. For the IF building (Figure 11) in dir.X as for the max $V_y$ on average the results between Modal and Rayleigh Damping with $K_{init}$ and $K_{comm}$ are very close, as $\zeta_n$ increases the Modal Damping compared to the two Rayleigh Damping approaches damps the shear less. Similar to dir. X, the same trends are also observed in the dir.Y.

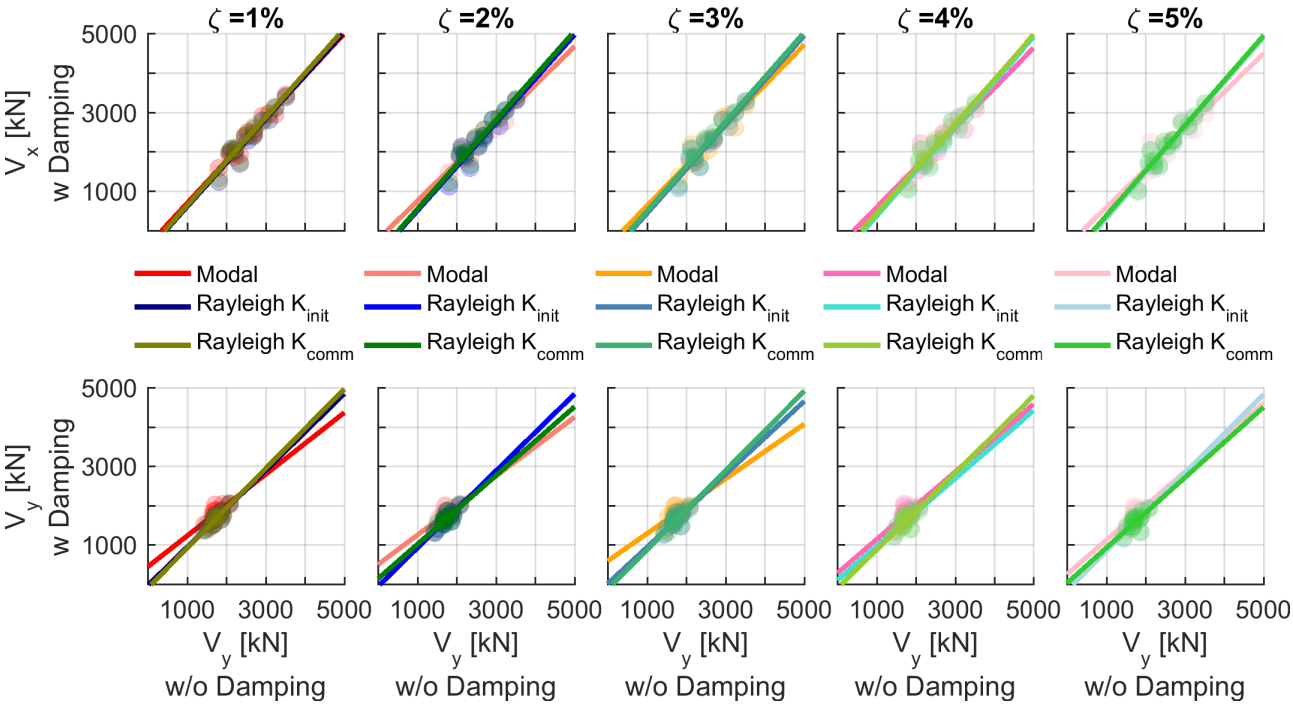


*Figure 11. Comparison of NRHAs for the BF model between Rayleigh and Modal Damping in terms of the maximum base shear in the X and Y directions (with trend lines)*

## 7. Summary and Conclusions

A 6-story reinforced concrete building designed for gravity loads only according to an old Italian building code is used as benchmark study to compare the effects of two different damping models on Nonlinear Response History Analyses. Two models are considered: with (IF) and without infills (BF). The two damping models considered are among the most used damping approaches found in the literature: Modal and Rayleigh damping. Damping rations ranging from 1% to 5% were considered.

Two variations of Rayleigh damping were used: with initial stiffness $K_{init}$ and with committed stiffness $K_{comm}$. NRHA analyses were performed for 20 pairs of ground motion records for a seismic intensity corresponding to return periods of 475 years. However, only 14 pairs were eventually used because of convergence issues with 6 record pairs. The Engineering Demand Parameters used for the comparisons are the maximum roof displacement at the center of mass (RD) and the maximum base shear Vy. The results show that between Modal Damping and Rayleigh Damping with $K_{init}$ or $K_{comm}$ the differences are low on average on BF and IF buildings.

This study indicates that even though differences emerge, the two EDPs, although not identical, are comparable when considering the overall set of analyses.

## 8. References


Ambraseys N, Smit P, Sigbjornsson R, Suhadolc P, Margaris B. (2002). Internet-site for European strong-motion data. European Commission, Research-Directorate General, Environment and Climate Programme.

Barbagallo F., Bosco M., Marino E. M., & Rossi P. P. (2020). On the fibre modelling of beams in RC framed buildings with rigid diaphragm, Bulletin of earthquake engineering, 18(1), 189-210.

Basaglia A., Cianchino G., Cocco G., Rapone D., Terrenzi M., Spacone E., & Brando G. (2021). An automatic procedure for deriving building portfolios using the Italian "CARTIS" online database, Structures (Vol. 34, pp. 2974-2986). Elsevier.

Cantagallo C.,Terrenzi M., Spacone E., Camata G. (2023) Structural demands obtained from real, scaled, spectral-matched and artificial accelerograms: analyses and comparisons, 18th World Conference on Earthquake Engineering, Milan, Italy

Cardone D., & Perrone G. (2015). Developing fragility curves and loss functions for masonry infill walls, Earthquakes and Structures, 9(1), 257-279

Carr A. J. (2007). RUAUMOKO Manual (Volume 1: Theory). University of Canterbury, Christchurch, New Zealand.

Charney, F. A. (2008). Unintended consequence of modeling damping in structures. J. Struct. Eng. 134, 581–592.

Chopra AK. (2012). Dynamics of Structures: Theory and Applications to Earthquake Engineering (4th edn), Prentice Hall: Englewood Cliffs, New Jersey.

Chopra A. K., & McKenna F. (2016). Modeling viscous damping in nonlinear response history analysis of buildings for earthquake excitation, Earthquake Engineering & Structural Dynamics, 45(2), 193-211.

Decanini L. D., & Fantin G. E. (1986). Modelos simplificados de la mampostería incluida en porticos. Caracteristicas de stiffnessy resistencia lateral en estado limite. Jornadas Argentinas de Ingeniería Estructural, 2, 817-836.

Eurocode 8 - Part 1: Eurocode 8. Design provisions for earthquake resistance of structures. Part 1-1: general rules – seismic actions and general requirements for structures. ENV 1998-1. Brussels: CEN; 2005.

ISTAT (2011) , Edifici residenziali ,http://daticensimentopopolazione.istat.it/Index.aspx?DataSetCode=DICA_EDIFICI1 (accessed September 14, 2023), in Italian.

Kent D. C., & Park R. (1971). Flexural members with confined concrete, Journal of the structural division, 97(7), 1969-1990.

Luzi L, Puglia R, Russo E. (2016). ORFEUS WG5. Engineering strong motion database, version 1.0. Istituto Nazionale di Geofisica e Vulcanologia, Observatories & Research Facilities for European Seismology.

Mazzoni, S., McKenna, F., Scott, M. H., & Fenves, G. L. (2006). OpenSees command language manual. Pacific earthquake engineering research (PEER) center, 264(1), 137-158.

Menegotto M., Pinto P. (1973). Method of analysis for cyclically loaded RC plane frames including changes in geometry and non-elastic behavior of elements under combined normal force and bending, Proceedings of IABSE Symposium on Resistance and Ultimate Deform ability of Structures Acted on by Well Defined Repeated Loads, 11:15-22.

Ministero dei lavori pubblici, Decreto ministeriale del 30/05/1974, Norme tecniche per la esecuzione delle opere in cemento armato normale e precompresso e per le strutture metalliche, Gazzetta ufficiale serie generale, 29/07/1974, Roma.

Noh, N. M., Liberatore, L., Mollaioli, F., & Tesfamariam, S. (2017). Modelling of masonry infilled RC frames subjected to cyclic loads: State of the art review and modelling with OpenSees. Engineering Structures, 150, 599-621.

Petracca M., Candeloro F., & Camata G. (2017). STKO user manual. ASDEA Software Technology: Pescara, Italy, 551.

Rayleigh L. (1945). The theory of sound, Dover: New York, NY.

Sassun K., Sullivan,T. J., Morandi P., & Cardone D. (2016). Characterising the in-plane seismic performance of infill masonry, Bulletin of the New Zealand Society for Earthquake Engineering, 49(1), 98-115.

Scott M. H., & Fenves G. L. (2006). Plastic hinge integration methods for force-based beam–column elements, Journal of Structural Engineering, 132(2), 244-252.

Spacone E., Filippou F. C., & Taucer F. F. (1996). Fibre beam-column model for non - linear analysis of R/C frames: Part I. Formulation, Earthquake Engineering & Structural Dynamics, 25(7), 711-725.

Spacone E., Filippou F. C., & Taucer F. F. (1996). Fibre beam-column model for non - linear analysis of R/C frames: part II. Applications, Earthquake engineering & structural dynamics, 25(7), 727-742.

Terrenzi M., Spacone E., & Camata,G. (2020). Comparison between phenomenological and fiber-section non-linear models, Frontiers in Built Environment, 6, 38.

Terrenzi M., Spacone E., & Camata G. (2022). Engineering demand parameters for the definition of the collapse limit state for code-conforming reinforced concrete buildings, Engineering Structures, 266, 114612

Wilson E. L., & Penzien J. (1972). Evaluation of orthogonal damping matrices, International Journal for numerical methods in engineering, 4(1), 5-10.